Pattern Recognition in Hyperspectral Imagery Using Spectral JTC

Mohammad S. Alam
Department of Electrical and Computer Engineering
University of South Alabama, Mobile, AL 36688-0002

Abstract

Pattern recognition in hyperspectral imagery is a challenging problem due to the minute nature of the target signature and the requirement to process huge amount of data. In this paper, we investigate the recent trends and advancements in joint transform correlation (JTC) based pattern recognition in hyperspectral imagery. In particular, we investigate the application of spectral fringe-adjusted JTC for efficient target recognition in hyperspectral imagery. Techniques for eliminating false target detection, minimizing effects of noise and other artifacts are considered. The performance of the spectral fringe-adjusted JTC has been compared with the existing techniques by generating ROC curves using real life hyperspectral datasets.

Key words: Pattern recognition, joint transform correlation, hyperspectral imaging

1. Introduction

Hyperspectral imaging spectometry is a new technology for remote sensing and target detection applications from airborne and spaceborne platforms. Hyperspectral sensors have been developed to provide sensor radiance spectrum corresponding to material characteristics [1-4]. Target detection is one of the fundamental tasks in hyperspectral image exploitation. Recently, several detection algorithms for hyperspectral imaging applications have been reported in the literature [1-4]. For example, an orthogonal subspace projection based classifier has been developed which can reduce dimensionality and helps in hyperspectral image classification [5]. The idea was to apply an orthogonal subspace projection classifier to eliminate all unwanted endmembers and interferences within a pixel, then use a matched filter to extract the desired endmember present in that pixel, which is very challenging to implement. Furthermore, orthogonal subspace projection becomes ineffective when the intrinsic dimensionality of data is less that the number of signatures present in the image. In hyperspectral imagery, generally the target is present in the form of a few pixels which makes it difficult to get the maximum likelihood estimates of the target class. This problem can be alleviated by using anomaly detection originally proposed by Reed and Xiaoli (RX) [6] where the detection decision is based on the maximum likelihood estimates of the background class. RX algorithm involves a practical detector, which does not rely on *a priori* information about the target. However, automatic thresholding, misclassifications and false alarms are the main challenges associated with this technique. If the target spectral signature is available as the reflectance spectra, the spectral angle mapper (SAM) algorithm can be used for detection purposes. However, the SAM technique provides good results only for targets having well separated distribution with small dispersions [4].

The performance of a target detection algorithm depends on the spatial information available corresponding to the target. One way to improve the detection accuracy is to introduce additional information about the target, such as the spectral information i.e., reflectance of the target at various wavelength bands. In the fringe-adjusted joint transform correlation (FJTC) [7-8] based detection algorithm for hyperspectral imagery, input spectral signatures from the unknown hyperspectral image are correlated with the reference signature using the FJTC technique [9]. The detection performance is sensitive to the shape of the target signature but not to its intensity, which makes the algorithm superior because the signature of a material is usually preserved whereas its intensity may change due to environmental conditions. This technique also yields very sharp and high correlation peaks corresponding to the targets.

In this paper, the performance of the spectral FJTC has been investigated and compared with existing techniques by generating ROC curves using real life hyperspectral datasets. The test results show that spectral FJTC is a viable alternative for pattern recognition in hyperspectral images when compared to alternate techniques.

Optics and Photonics for Information Processing III, edited by Khan M. Iftekharuddin, Abdul Ahad Sami Awwal,
Proc. of SPIE Vol. 7442, 74420M · © 2009 SPIE · CCC code: 0277-786X/09/$18 · doi: 10.1117/12.830779

2. Spectral FJTC

Joint transform correlation (JTC) technique has been found to be an effective detection technique for two-dimensional pattern recognition applications [7,8]. The fringe-adjusted JTC (FJTC) technique has been found to yield better correlation peak compared to other existing techniques [7]. To provide efficient target detection in case of hyperspectral images involving challenging targets such as single pixel targets, the spectral FJTC (SFJTC) technique can be used. When the input scene contains only one spectral signature, the correlation output produced in a JTC technique includes three terms, a strong dc or zero-order term at the center flanked by a pair of cross correlation terms in the correlation array. The FJTC technique provides enhanced correlation performance, where the joint power spectrum is multiplied by a real-valued filter, called the fringe-adjusted filter (FAF) before applying the inverse Fourier transform to yield the correlation output. Thus the technique overcomes the problem of zero-order correlation term and produces sharp delta-function-like correlation peaks [7].

In the spectral FJTC technique, the reference spectral signature $r(x+x_0)$ and the unknown input spectral signature $\tilde{t}(x-x_0)$, are introduced in the input plane by separating them with a distance of $2x_0$ along the x axis. The input joint signature $f(x)$ can be expressed as

$$f(x) = r(x + x_0) + t(x - x_0) \tag{1}$$

Applying Fourier transform operation to Eq. (1), we get

$$F(u) = |R(u)| \exp[j\phi_r(u)] \exp(jux_0) + |T(u)| \exp[j\phi_t(u)] \exp(-jux_0) \tag{2}$$

where $|R(u)|$ and $T(u)$ are the amplitudes, and $\phi_r(u)$ and $\phi_t(u)$ are the phases of the Fourier transform of $r(x)$ and $t(x)$, respectively. The intensity i.e., the joint power spectrum (JPS) corresponding to Eq. (1) as given by

$$\begin{aligned} |F(u)|^2 &= |R(u)|^2 + |T(u)|^2 + |R(u)||T(u)|^* \exp\left[j\{\phi_r(u) - \phi_t(u) + 2ux_0\}\right] \\ &\quad + |R(u)|^* |T(u)| \exp\left[j\{\phi_t(u) - \phi_r(u) - 2ux_0\}\right] \end{aligned} \tag{3}$$

In Eq. (3), the first two terms correspond to the zero-order terms and the last two terms are the desired cross correlation between the reference signal and the input signal. To eliminate the zero-order terms, we utilized the Fourier plane image subtraction technique [8], where the input-scene-only power spectrum and the reference-image-only power spectrum are subtracted from the JPS of Eq. (2). Thereafter, the modified JPS can be expressed as

$$\begin{aligned} |I(u)|^2 &= |F(u)|^2 - |R(u)|^2 - |T(u)|^2 \\ &= |R(u)||T(u)|^* \exp\left[j\{\phi_r(u) - \phi_t(u) + 2ux_0\}\right] + |R(u)|^* |T(u)| \exp\left[j\{\phi_t(u) - \phi_r(u) - 2ux_0\}\right] \end{aligned} \tag{4}$$

It may be mentioned that a classical JTC technique yields large correlation sidelobes and large correlation peak width [9, 10], which deteriorates the detection performance. To provide sharp correlation peaks and low correlation sidelobes, the FJTC technique is used in this work, where the modified JPS found in Eq. (4) is multiplied by a fringe-adjusted filter (FAF) before applying the final inverse Fourier transform operation. The FAF is characterized by a transfer function, defined as

$$H(u) = A(u)\left[B(u) + |R(u)|^2\right]^{-1} \tag{5}$$

where $A(u)$ and $B(u)$ are either constants or functions of u. When $A(u) = 1$ and $|R(u)|^2 \rangle\rangle B(u)$, the FAF can be approximated as

$$H(u) \approx |R(u)|^{-2} \tag{6}$$

Finally, the inverse Fourier transformation of the filtered modified JPS yields the correlation output, given by

$$C(x) = F^{-1}\left\{H(u) \times \left|I(u)\right|^2\right\} \tag{7}$$

In case of hyperspectral image cubes, one deals with *n* dimensional vectors, $x = \left[x_1, x_2, \ldots. x_n\right]^T$ called the pixel vectors, where each pixel vector undergoes the correlation process described in the previous Section. Now if we record the highest correlation peak to identify the location of an input signature, we may not obtain distinguishable correlation performance since the highest peak values in the correlation output with true signature and those with false signature do not usually differ much. In this paper, we used a postprocessing step which involves the application of a decision metric. Decision fusion results remains the same even if the target reflectance at all wavelength bands drops or increases by some constant $k > 0$, making this method sensitive to spectral shape rather than intensity. A flowchart showing the various steps involved in the spectral FJTC algorithm is shown in Fig. 1.

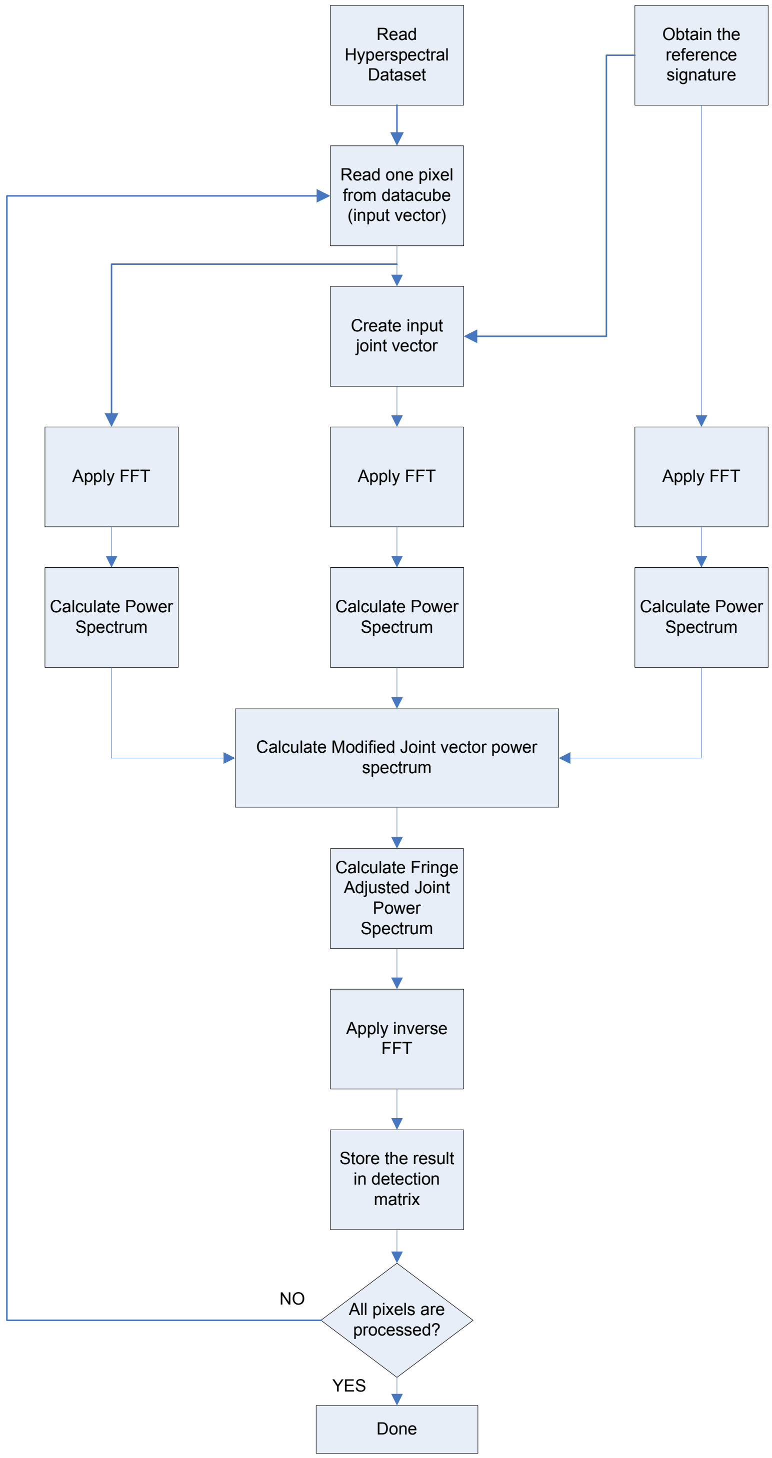

Fig. 1. Spectral FJTC flowchart.

3. Test Results

To investigate the performance of the SFJTC technique, two hyperspectral datasets, HYDICE terrain data and CASI battleship park data with corrupted target signatures manually inserted into the scenes, were used. The calibrated

HYDICE cube consists of 210 bands with a spectral resolution of about 10 nm. About 75 of these bands were in the water absorption region, containing sensor errors. However, negative intensities were removed to avoid unnecessary errors. The calibrated CASI data cube consists of 36 bands ranging from 433.7 nm to 965 nm. Spectral variability was introduced in two different ways. First, each inserted corrupted signature is generated by multiplying the pure target signature by a percentage to determine the proportion of the target signature for each inserted pixel. For example, if the percentage for a given corrupted target signature is 55%, then, the pure target signature is multiplied by a factor of 0.55, and the signature for the background of that pixel location is multiplied by a factor of 0.45, and the two are added together. This type of spectral variability simulates spectral mixing of target and background signatures, which is a challenge in hyperspectral imaging based target detection.

Figure 2 shows the results obtained by using the spectral FJTC technique with HYDICE data. Figure 2(a) represents one band of the HYDICE data cube, Fig. 2(b) represents the truth mask, Fig. 2(c) represents the correlation output obtained using the spectral output, and Fig. 2(d) depicts the 3D version of Fig. 2(c). There are ten targets as shown in the truth mask plot, where all of these targets are successfully detected by the proposed technique as shown in the correlation output. Similarly, for CASI data, the spectral FJTC technique effectively detects all of the ten targets as depicted in Fig. 3.

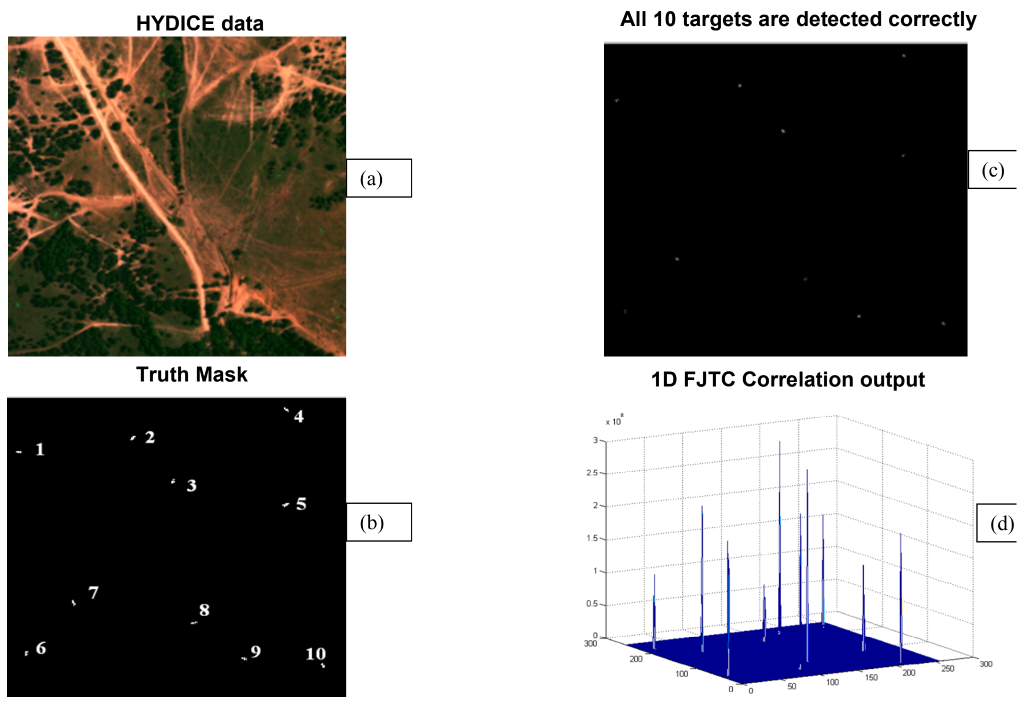

Figure 2. Performance of 1D-FJTC using HYDICE data

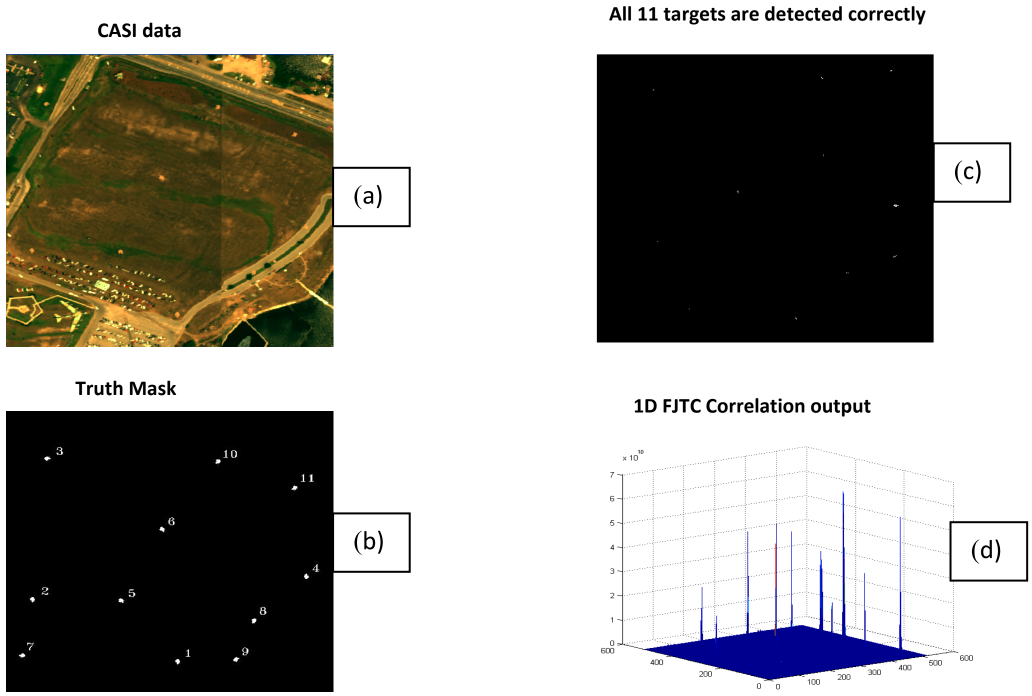

Figure 3. Performance of the spectral FJTC using CASI data.

4. PERFORMANCE COMPARISON

We investigated the performance and advantages and disadvantages of spectral FJTC as well as other existing algorithms for target detection in hyperspectral imagery. To investigate the performance of the various algorithms, receiver operating characteristics (ROCs) curves were used [10]. To compare the detection performance of the spectral FJTC algorithm against other algorithms (e.g., RX, PARRX, etc.), 12 datasets were used such as CASI-B01, CASI-B03, HYDICE-B01 and HYDICE-B03, respectively. Each of the aforementioned 4 datasets involved three cases: noise-free (NoNoise), 5% noisy (Noise5) and 10% noisy (Noise10) cases, thus making a total of 12 datasets.

Figures 4 to 7 show the results of the above mentioned algorithms for the 12 datasets, where CASI is denoted as CS, HYDICE is denoted as HY, respectively. In the ROC curves of Figs. 4 to 7, lines and blank square ticks is used for spectral FJTC (denoted as sp… in the plot). From Figs. 4 to 7, it is evident that the spectral FJTC algorithm shows excellent performance compared to alternate and/or existing algorithms and it is a viable alternative for target detection in hyperspectral imagery.

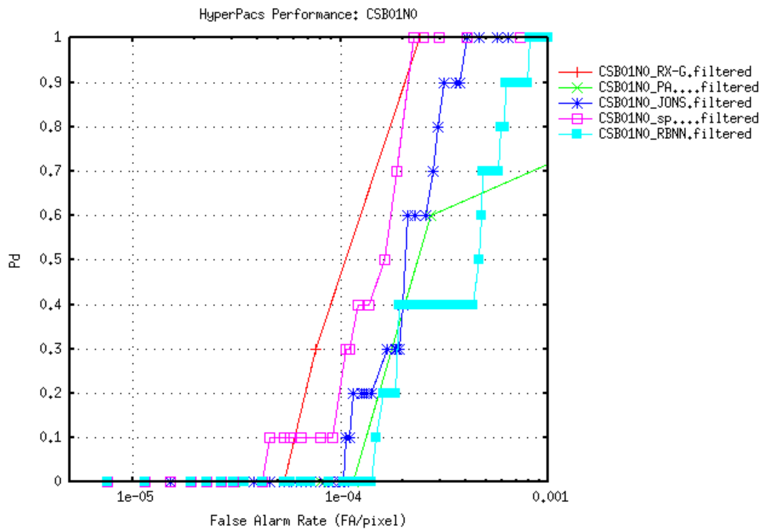

HyperPacs Performance: CSB01N0
Pd
False Alarm Rate (FA/pixel)
1e-05
1e-04
0.001
CSB01N0_RX-G.filtered
CSB01N0_PA....filtered
CSB01N0_JONS.filtered
CSB01N0_sp....filtered
CSB01N0_RBNN.filtered

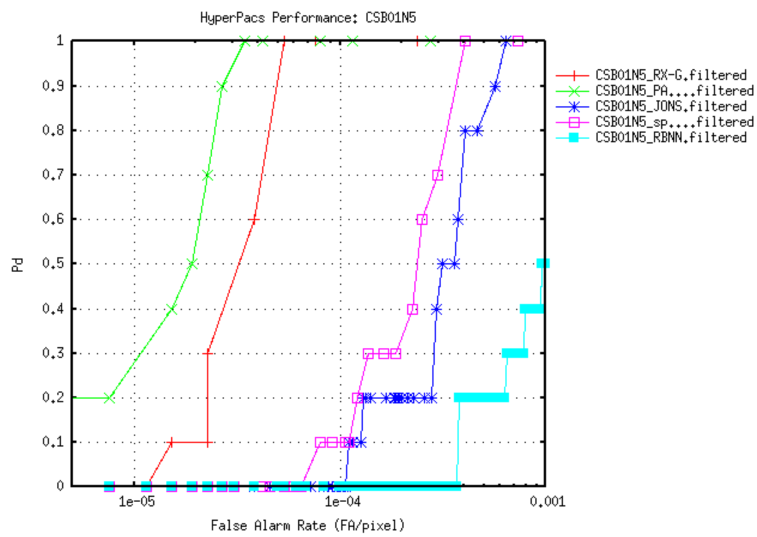

HyperPacs Performance: CSB01N5
Pd
False Alarm Rate (FA/pixel)
1e-05
1e-04
0.001
CSB01N5_RX-G.filtered
CSB01N5_PA....filtered
CSB01N5_JONS.filtered
CSB01N5_sp....filtered
CSB01N5_RBNN.filtered

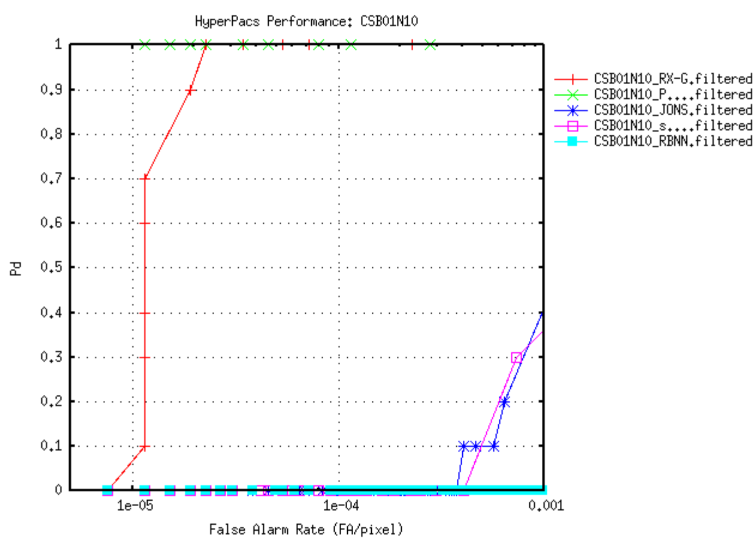

HyperPacs Performance: CSB01N10
Pd
False Alarm Rate (FA/pixel)
1e-05
1e-04
0.001
CSB01N10_RX-G.filtered
CSB01N10_P....filtered
CSB01N10_JONS.filtered
CSB01N10_s....filtered
CSB01N10_RBNN.filtered

Figure 4. ROC detection performance for CASI B01 dataset (NoNoise, Noise5, and Noise10 cases).

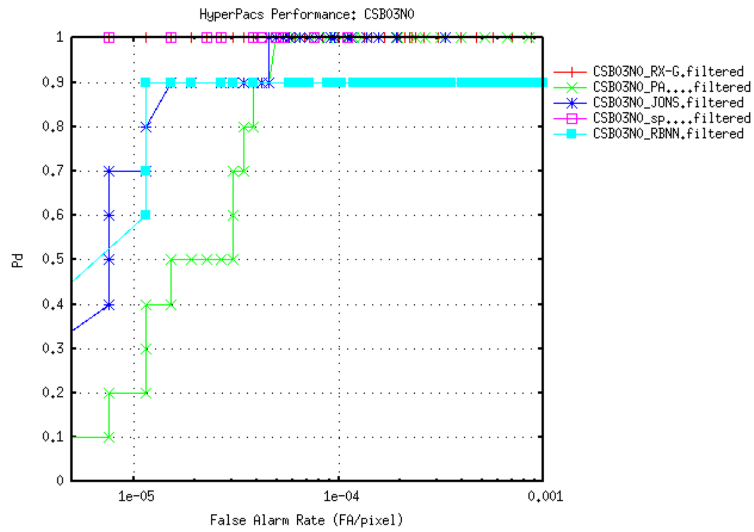

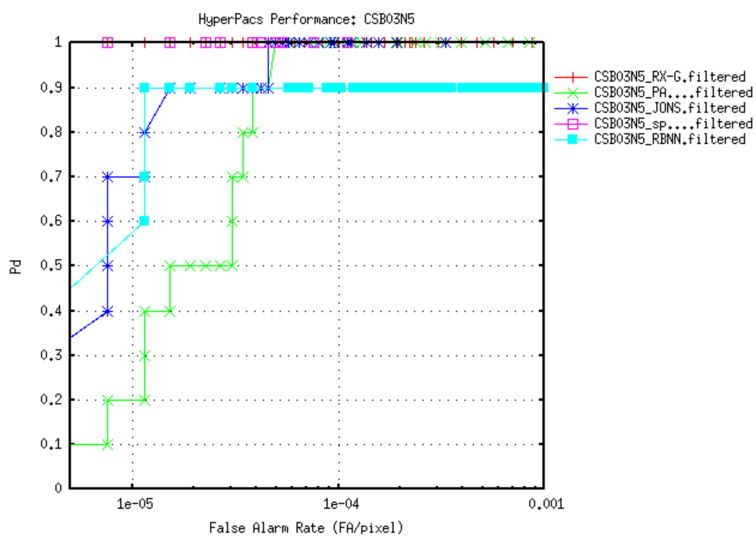

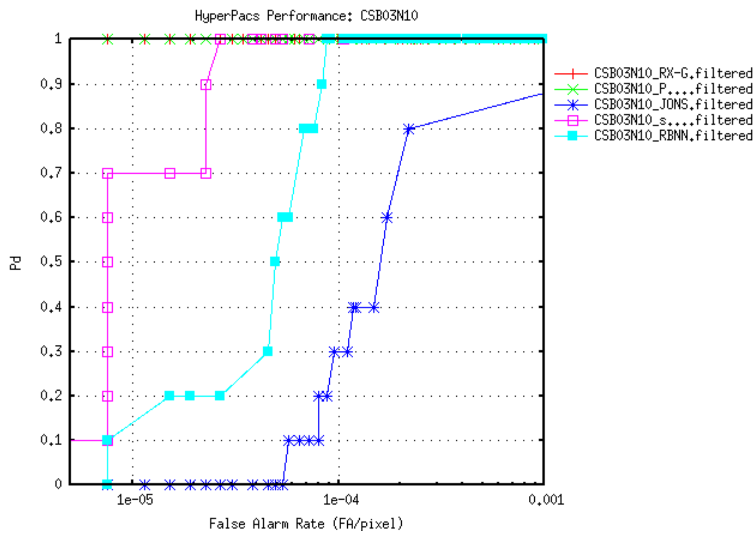

Figure 5. ROC detection performance for CASI B03 dataset (NoNoise, Noise5, and Noise10 cases).

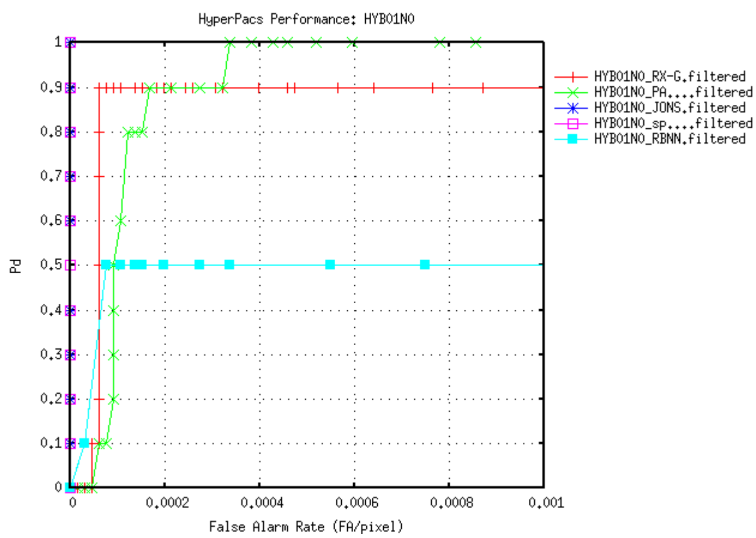

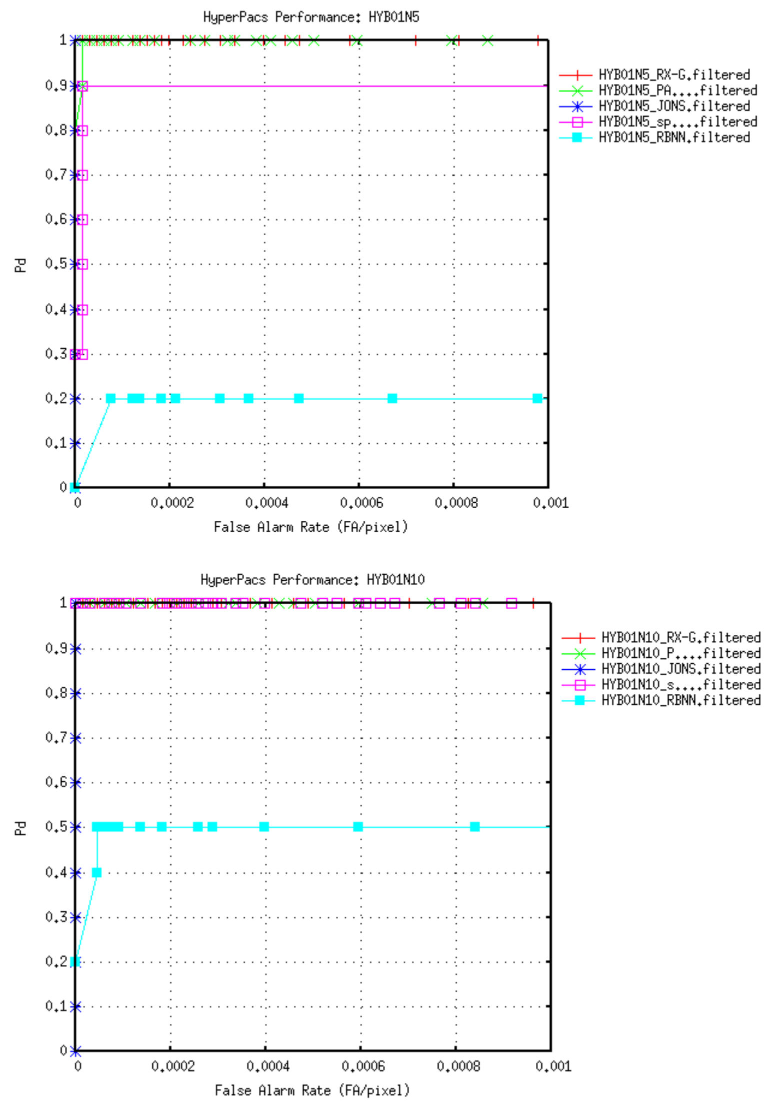

Figure 6. ROC detection performance for HYDICE B01 dataset (NoNoise, Noise5, and Noise10 cases).

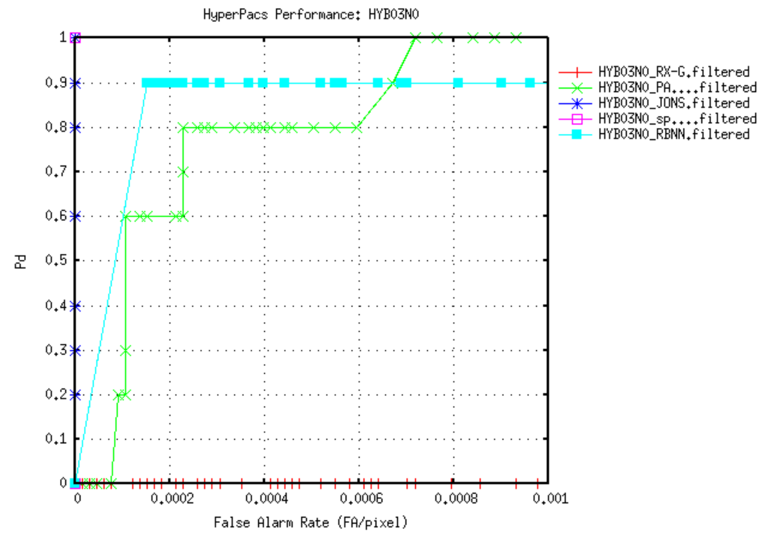
HyperPacs Performance: HYB03N0
Pd
False Alarm Rate (FA/pixel)
HYB03N0_RX-G.filtered
HYB03N0_PA....filtered
HYB03N0_JONS.filtered
HYB03N0_sp....filtered
HYB03N0_RBNN.filtered

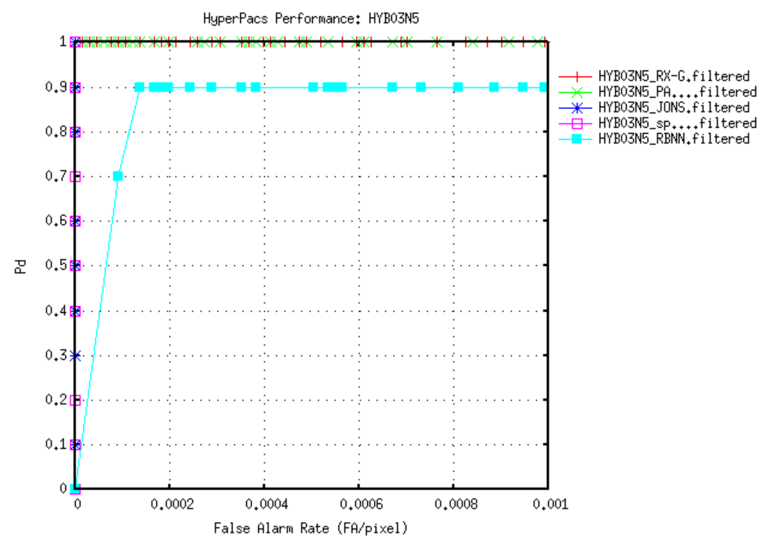
HyperPacs Performance: HYB03N5
Pd
False Alarm Rate (FA/pixel)
HYB03N5_RX-G.filtered
HYB03N5_PA....filtered
HYB03N5_JONS.filtered
HYB03N5_sp....filtered
HYB03N5_RBNN.filtered

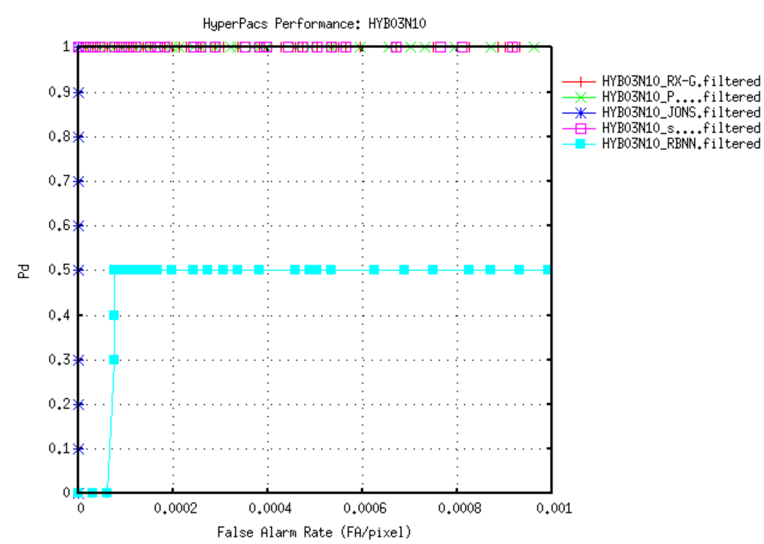
HyperPacs Performance: HYB03N10
Pd
False Alarm Rate (FA/pixel)
HYB03N10_RX-G.filtered
HYB03N10_P....filtered
HYB03N10_JONS.filtered
HYB03N10_s....filtered
HYB03N10_RBNN.filtered

Figure 7. ROC detection performance for HYDICE B03 dataset (NoNoise, Noise5, and Noise10 cases).

5. CONCLUSION

In this paper, we investigated the performance of all major algorithms available in the literature for hyperspectral target detection applications. We utilized the ROCs to compare the performance of various algorithms. After analyzing the performance of various existing and newly developed algorithms, we found that the spectral FJTC algorithm yields better performance, especially for improving the probability of target detection and reducing the false alarm rate.

6. ACKNOWLEDGEMENT

The author wish to thank S. Ochilov, E. Sarigul and A. Sakla for many rewarding discussions.

7. REFERENCES

1. D. Manolakis, D. Marden and G. Shaw, "Hyperspectral image processing for automatic target detection applications," Lincoln Laboratory Journal, vol. 14, p. 79-114, 2003.
2. D. Slater and G. Healey, "A spectral change space representation for invariant material tracking in hyperspectral images," Proceedings of SPIE, vol. 3753, p. 308-317, 1999.
3. M. S. Alam and S. Ochilov, "Adaptive hyperspectral band selection," Proc. SPIE, vol. 5908, pp. 301-308, 2005.
4. D. Manolakis and G. Shaw, "Detection algorithms for hyperspectral imaging applications," IEEE Signal Processing Magazine, vol. 19, p. 29 – 43, 2002.
5. A. Chowdhury and M. S. Alam, "Target detection in hyperspectral imagery using NAPCA/PCA and an OSP based ratio," *Proc. SPIE*, Vol. 6365, p. 63650(1-6), Stockholm, September 11-14, 2006.
6. I. S. Reed and X. Yu, "Adaptive multiple-band CFAR detection of an optical pattern with unknown spectral distribution," IEEE Trans. Acoustics, Speech, and Signal Processing, vol. 38, pp. 1760-1770, 1990.
7. M. S. Alam and M. A. Karim, "Fringe-adjusted joint transform correlation," Applied Optics, vol. 32, p. 4344-4350, 1993.
8. M. S. Alam, A. Bal, E. H. Horache, S. F. Goh, C. H. Loo, S. P. Regula and A. Sharma, "Metric for evaluating the performance of joint-transform-correlation-based target recognition and tracking algorithms," Optical Engineering, vol. 44, p. 067005, 2005.
9. M. S. Alam and S. Ochilov, "Target detection in hyperspectral imagery using one-dimensional fringe-adjusted joint transform correlation," *Proc. SPIE*, Vol. 6245, p. 624505(1-11), Orlando, April 17-21, 2006.
10. D. R. Parker, S. C. Gustafson and T. D. Ross, "Receiver operating characteristic and confidence error metrics for assessing the performance of automatic target recognition systems," Optical Engineering, vol. 44, p. 097202, 2005.